https://doi.org/10.5194/egusphere-2023-2501
Preprint. Discussion started: 10 November 2023

The Dynamic Effect of Root Exudates on Soil Structure: Aggregate Stability and Packing

Maoz Dor[1*], Itamar Assa[2*], Yael Mishael[2]

[1]Department of Soil, Plant, and Microbial Sciences, Michigan State University, East Lansing, MI 48824, USA
[2] Department of Soil and Water Sciences, The Robert H. Smith Faculty of Agriculture, Food and Environment, The Hebrew University of Jerusalem, Rehovot, 7610001, Israel
* Equally contributing authors

Correspondence to: Maoz Dor (dormaoz@msu.edu)

Abstract

The importance of soil structure, packing and stability, cannot be overstated as it controls vital processes in the terrestrial environment. Physical, chemical and biological processes altogether affect the dynamics of soil structure with the biological driver being the most complex and least explored. We quantified, developing and applying advanced methods, the effect of mucilage (0.035% w/w), the main substance in root exudates, on soil packing and stability, by micro-CT and laser granulometry (aggregate durability index), respectively. Upon mucilage addition to soils, or plant growth, soil aggregate size and aggregate stability both increased, however, the intensity varied between the soils, in the order of sandy-clay-loam > loamy-sand > clayey soils. Scanning electron microscope and X-ray diffraction measurements focusing on the smaller soil aggregates (<250 µm) and their mineralogy, bring forward their dominant role in aggregation and stabilization processes induced by mucilage. The complex effects of mucilage coupled with a physical driver, wetting and drying, on microorganism activity, were explored. Compensating microorganism activities, root mucilage consumption and self-mucilaginous polysaccharides production, most likely explain the stability steady state reached within three days. The presence of mucilage in sandy-clay-loam and clayey soils, intensified and overcame the aggregation and disaggregation induced by wetting and drying, respectively. Elucidating soil structure dynamics will enable better understanding of soil stability processes and thereby develop better strategies for soil erosion management.

Keywords: Soil structure, Mucilage, Imaging, Aggregate stability

1 Introduction

To address one of the most urgent environmental challenges, soil structure erosion, one must seek an in-depth understanding of the drivers, mechanisms, and rates, of soil aggregation processes at the field scale but also at the micron scale at which the fundamental processes occur. Soil structure is a key factor in many processes, including water retention and infiltration, gas exchange, soil organic matter and nutrients dynamics, microbial activity and soil erosion (Lal, 2001; Young and Crawford, 2004; Ball, 2013; Christensen, 2001; Bronick and Lal, 2005; Hadas and Stibbe, 1977; Pardo et al., 2000; Alletto et al., 2012;

Assouline and Mualem, 1997). Water-stable aggregates in well-structured soils improve water infiltration, better withstand rainfall impacts, and reduce surface runoff and erosion (Barthès and Roose, 2002; Cantón et al., 2009; Levy and Mamedov, 2002; Nciizah and Wakindiki, 2015).

Soil structure is viewed from two perspectives, the spatial arrangement of the soil particles into an aggregated system (Tisdall and Oades, 1982; Totsche et al., 2018; Yudina and Kuzyakov, 2023), and/or the spatial configuration of the pore network induced by biological and physical mixing processes (Baveye et al., 2022; Rabot et al., 2018; Vogel et al., 2022). Due to the disruption of soil structure caused by tillage and other agronomic operations, agricultural top soils can be well described by the aggregates perspective (Or et al., 2021). The aggregates perspective describes how mineral particles combine with organic and inorganic substances to form hierarchical structures through binding agents such as oxides and clay minerals, hyphae, extracellular polymeric substances, and root exudates (Tisdall and Oades, 1982; Totsche et al., 2018). Soil structure changes constantly in space and time due to direct and indirect physical, chemical and biological processes (Totsche et al., 2018). In the current study we focus on the effect of root exudates, a biochemical driver, on soil structure. Virtually all plants exude about 25% of their total photosynthetic output into the rhizosphere, of which approximately half is in the form of mucilage, a gelatinous high-molecular-weight substance consisting mainly of polysaccharides (Ahmed et al., 2014; Chaboud and Rougier, 1984; Walker et al., 2003). Apart from mucilage's role in plant physiology it directly affects soil structural, packing and stability (Morel et al., 1991).

Packing and stability of soils are two key parameters that determine soil structure. Soil packing is the arrangement of solids particles and aggregates into a system of inter/intragranular voids, whereas stability refers to the capacity to retain this packing under different stresses (Amézketa, 2008a; Cerdà, 1998). Previous studies have shown that mucilage, originated from both roots and soil bacteria, plays a central role in stabilizing the soil rhizosphere, mainly by strengthening inter-aggregates pores within soil aggregates which represent structural planes of weakness (Oades, 1993). Similar observations were made by Morel et al. (1991, 1987) where maize root mucilage was readily adsorbed on clay minerals and exerted an immediate and significant increase in soil aggregate stability in silty clay and silt loam soils. Furthermore, root mucilage analogue was found to better stabilize soil than bacterial mucilage, upon the disruptive effect of wetting and drying by decreasing wetting rate due to repellency (Czarnes et al., 2000; Popović and Cerdà, 2023).

Most of these studies examined a single soil and did not monitor the effect of mucilage on both stability and packing, which are clearly coupled. More importantly, the tested mucilage concentrations were significantly higher than the typical rhizosphere concentrations, which do not represent realistic environmental conditions. Finally, technological advances of recent decades have enabled us to characterize in-situ the changes in soil stability and packing induced by mucilage, at the micron scale.

In this study we thoroughly characterize how mucilage affects soil stability and packing of three different agricultural soils, clayey, sandy-clay-loam, and loamy-sand soils, from different climate zones. To characterize soil packing, we measured soil aggregate distribution by micro-CT and developed a methodology based on scanning electron microscopy (SEM) which enabled better imaging and analysis at the sub-micron scale. To quantify soil stability, we applied our recently developed aggregate durability index (ADI) (Dor et al., 2019). We hypothesize that mucilage promotes soil aggregation, leading to an increase in soil stability, however the degree of this effect may vary depending on soil texture. To shed light on the complexity and dynamics of soil structure, we not only investigate the effects of mucilage, but also the effect of wetting and drying, on soil stability and soil microbial activity.

2 Materials and Methods

2.1 Soils

Soils were collected from 0-20 cm depth at uncultivated sites found in Mediterranean and semi-arid climate zones, representing the major agricultural areas in Israel. The sampled soils varied in textures and were named accordingly: Vertisol (Ein Harod clay), Loess (Mishmar Hanegev sandy-clay-loam), and Hamra (Rehovot sandy soil) (Table 1). Soil samples were air-dried, passed through a 2-mm sieve, and selected physical and chemical properties of the soils were determined by standard analytical methods (Gee and Or, 2002; Loeppert and Suarez, 1996).

2.2 Soil minerology

The mineralogy of the soils was assessed by x-ray diffraction (XRD). Soil samples were spiked with 20% wt. corundum (Al2O3), mixed and loaded into X-ray diffraction (XRD) sample holder by front loading followed by razor blade leveling. XRD patterns were acquired in Bragg-Brentano geometry using a PANalytical X'Pert diffractometer with CuKα radiation operated at 45 kV and 40 mA. The samples were scanned from 5 to 70° 2θ at a step size of 0.013° 2θ, using a PIXcel detector in continuous scanning line (1D) mode with an active length of 3.35°. Mineral phase identification was performed using HighScore Plus® software based on ICSD database. Quantitative approximations of mineral phase abundances were performed using FullPat program (Chipera and Bish, 2002).
Furthermore, to analyze the speciic mineralogy of the clay fraction (<2 μm) the following steps were taken: 1) carbonate minerals and salts were removed using buffered acetic acid; 2) samples were Sr saturated; and 3) A low-intensity ultrasonic treatment was used to disaggregate samples. The clay fraction was then collected from suspensions according to Stokes Law. The collected clay suspensions were pipetted onto glass slides and analyzed after air-drying, glycolation (at least 8 h at 60 °C and cooling overnight), and heating for 2 h to 550 °C (Moore and Reynolds, 1989). XRD patterns were acquired in Bragg-Brentano geometry using a PANalytical X'Pert diffractometer with CuKα radiation operated at 45 kV and 40 mA. Samples were scanned from 2 to 30° 2θ with a step size of 0.013° 2θ using a PIXcel detector in continuous scanning line (1D) mode with an active length of 1°. Semi-quantitative clay abundances were estimated from the relative peak areas of I-S, kaolinite, illite and chlorite following the method of (Biscaye, 1965).

https://doi.org/10.5194/egusphere-2023-2501
Preprint. Discussion started: 10 November 2023

2.3 Mucilage extraction

In this study, mucilage was extracted from Chia seeds (*Salvia hispanica L.*) and used as an analogue for rhizosphere mucilage, owing to its chemical composition being comparable to maize root exudates (Carminati and Vetterlein, 2013; Kroener et al., 2014). The extraction followed a protocol reported by Capitani et al. (2013). Briefly, chia seeds were immersed in deionized water in a 1:10 ratio by mass for 4 hours at 27°C. Samples were then freeze-dried and passed through an 800 µm sieve.

2.4 Soil sample preparation

To measure the effect of mucilage on soil structure, two treatments were examined: untreated soil denoted 'control', and soil to which mucilage was added denoted 'mucilage' (three replicates for each treatment). To add mucilage to the soil, a suspension of dried mucilage in deionized water was prepared and applied to the soil samples, resulting in a volumetric water content of 50% and a concentration of 0.35 mg dry mucilage per g of dry soil. This concentration is consistent with the range of mucilage concentrations typically found in the rhizosphere, as reported in previous studies (Chaboud, 1983; Zickenrott et al., 2016; Holz et al., 2018). The control treatment consisted of adding only deionized water to achieve the same volumetric water content. To regain their initial moisture content, soil samples were dried at ambient conditions for 7 days after each treatment.

Another experimental factor assessed was the impact of soil water content (WDC), incorporated into a factorial design along with the mucilage and control treatments. Soil WDC carried out by slow irrigation of the soil samples with distilled water, using a nozzle syringe. The samples were subsequently dried in an oven at 40°C to simulate the hot season conditions at the collection site, until they returned to their original air-dried weight (Gao et al., 2007; Potchter et al., 2008).

2.5 Soil packing measurements

The effect of mucilage on soil packing was characterized by the analysis of 3D and 2D soil images, obtained by micro-CT (Sky-scanner 1174, Bruker, Belgium) and scanning electron microscope (JEOL It 100 Low vacuum; SEM), respectively.

2.5.1 3D – Micro-CT analysis

For the micro-CT analysis, Hamra Loess and Vertisol soil samples were loosely packed in a cylindrical polycarbonate column (d=15 mm x h=40 mm). Each soil sample was scanned twice, pre and post mucilage addition providing two sets of images of the same soil sample. The X-ray source was set at 80 kV and 100 mA. A total of 1105 projections were obtained for each sample with an exposure time of 2.2 s and an isotropic voxel size of 9 μm^3. The NRecon software (NRecon® Skyscan® software, version 1.6.1.2, Bruker, Belgium) was used to reconstruct the X-ray projections into a 16-bit grayscale tiff stack. 3D image processing was carried out by FIJI (Schindelin et al., 2012). In order to enhance the accuracy of image segmentation a pre-processing procedure was perform, which included denoising by a 3D median filter, and calibration of the grayscale based on the percentiles of the pore and solid phases intensity peaks (Koestel, 2018). This approach facilitated a more reliable thresholding of the images using the Otsu method (Otsu, 1979) ultimately resulting with binary images depicting pore and solid phases in each soil sample. To determine the aggregate size distribution, the maximum inscribed sphere algorithm was implemented on the binary image of the solid phase. This algorithm calculates the local thickness for each voxel by finding the diameter of the largest inscribed sphere that can fit within the image foreground. (Doube et al., 2010). The aggregate size distribution was then calculated by a kernel density estimation (KDE) implemented within the SciPy library (Virtanen et al., 2020). To estimate the effect of mucilage on soil structure the difference between the aggregate size distributions of the two treatments was calculated, (i.e. the aggregate size distribution of the mucilage treatment minus the control). The degree of soil aggregation was then determined by calculating the area under the positive range of the resulting distribution difference. It should be noted that in this context aggregate size distribution encompasses both soil particles and aggregates, as they cannot be differentiated solely through imaging methods.

2.5.2 2D – Scanning Electron Microscopy

For the SEM analysis, soil samples (pre and post mucilage addition) were first passed through a 250 µm sieve and mounted on 30 mm round SEM aluminum stubs using adhesive carbon tape. Secondary electron images were obtained using the following operating conditions: 20 keV, 10 mm WD, resolution of 2560 x 1920 pixels, x40 magnification for the Hamra soil (pixel size of 0.0625 μm^2) and x200 magnification for the Loess and Vertisol soils (pixel size of 1.56 μm^2). A total of 180 images were acquired for each soil, consisting of 90 pre-mucilage addition and 90 post-mucilage addition images. Segmentation process was obtained by pixel classification process, using Ilastik (Berg et al., 2019), followed by Gaussian smoothing filter and particle analysis process using FIJI (Schindelin et al., 2012). Finally, aggregate size distribution was calculated using the same method described earlier.

2.6 Soil stability measurements

Soil stability was assessed using our recently developed aggregate durability index (ADI) (Dor et al., 2019). Briefly, aggregate size distribution was measured using laser granulometry (Mastersizer 3000; malvern instruments, UK) before and after sample sonication. Laser granulometry is used to measure aggregate size distribution that involves passing a laser beam through a dispersed particle suspension and analyzing the scattered light patterns that arise from the diffraction of light by the particles. The ADI provides the difference between the water-stable and disaggregated (by sonication) aggregate size distribution of the sample. To further investigate the effect of mucilage on aggregate size fraction stability, each of the soil samples was sieved to four soil aggregate size fractions: <50, 50-100, 100-250 and 250-2000 µm, followed by ADI measurements (see section 2.4). Additionally, we conducted wet sieving of the soil samples to determine the water-stable aggregate mean weight diameter (MWD), which is a commonly used method to evaluate soil aggregate stability (Shukla et al., 2006; Le Bissonnais et al., 2018; Bavel, 1950). Briefly, 4 g of the soil samples (<2 mm) were placed on the topmost of a stack of sieves with descending mesh size (2, 1, 0.5, 0.25 and 0.106 mm) from top to bottom. The samples were first

https://doi.org/10.5194/egusphere-2023-2501
Preprint. Discussion started: 10 November 2023

immersed in distilled water and then sieved by moving the sieve set vertically. The soil retained by each sieve was dried at 40 °C for 24 h (reaching air-dried wet), weighed and corrected for oven-dried weight (according to the soils pre-determined Hygroscopic moisture content).

2.7 Soil Microorganisms activity

To assess the bioactivity of soil, respiration is commonly used as a general indicator. The emission of CO_2 was measured by the titration technique in which alkali reacts chemically with CO_2 and can be titrated with acid to an endpoint which is relative to the amount of CO_2 released by soil microorganisms (Bartha and Parmer, 1965). 60 gr of soil (pre and post mucilage addition) was placed in a 1L glass jar along with a vial of 2 ml of 1N NaOH and was incubated at 27°C for 7 days. Following incubation, 2 ml of 3N $BaCl_2$ was added to the NaOH solution for the precipitation of CO_2 and 100 µl of phenolphthalein were added as pH indicator. Finally, NaOH solution was titrated with 0.5N of HCl to determine the amount of CO_2 emission. Control jars without soil were included in the experiment to correct the CO_2 level in the jar at the start of the incubation.

2.8 In-situ stability

To evaluate the *in-situ* effect of root exudates on soil stability, chia plants were grown in the three saturated tested soils at 25°C for 14 days, packed in cylindrical polycarbonate columns (d=15 mm x h=40 mm). Thirty chia seeds were planted in each column, leading to a high root density in the soil, which served as the 'rhizosphere soil' treatment. The columns were watered with deionized water daily from the top. Control treatments were also set up under the same conditions but without chia seeds and referred to as 'bulk soil' treatment. Each treatment had three replicates. At the conclusion of the 14-day growth period, soil samples were collected from the center of the columns designated for the "bulk soil" treatment. For the "rhizosphere soil" treatment, samples were obtained from the soil that adhered to the roots at the center of the columns. Subsequently, soil stability analysis using ADI was conducted in accordance with the procedure outlined in section 2.3.

2.9 Statistical analysis

The significance for all tested effects on soil stability was assessed by a one-way ANOVA (for each of the three tested soils), except of the effect of mucilage treatment and soil aggregate size fractions on soil stability, which was assessed by two-way ANOVA. The effect of WDC on the contribution of mucilage on soil stability followed by a post hoc Tukey test. All the statistical analysis was carried by JMP®, Version 16. SAS Institute Inc.

https://doi.org/10.5194/egusphere-2023-2501
Preprint. Discussion started: 10 November 2023

3 Results and Discussion

3.1 Effect of mucilage on soil packing

3.1.1 Imaging soil particles binding by mucilage

To directly image mucilage in the rhizosphere is very challenging since the environmental concentrations are relatively low ~0.035% (w/w) (Chaboud, 1983; Holz et al., 2018; Zickenrott et al., 2016). To the best of our knowledge, for the first time, the interactions (binding) of soil particles following mucilage addition at such low concentrations were captured by SEM images (Fig. 1). Two main binding configurations were observed (for the Hamra and the Loess soils), strings (Fig. 1 a,c) and webs (Fig. 1 b,d) suggesting mucilage forms various bridging modes between soil particles forming aggregates. These images imply that the addition of mucilage to the soil acts as a binding agent that prompts the soil particles together, triggering aggregation processes in the soil, and therefore an overall increase in aggregate sizes, post aggregation, is expected. Furthermore, we hypothesize that mucilage-induced aggregation would increase soil stability.

3.1.2 Effect of mucilage on soil aggregate size distribution

Aggregate size distributions of the three tested soils, pre and post mucilage treatment, were measured and analyzed from micro-CT and SEM images and presented as the relative volume or area ratio vs. aggregate size (Fig. 2). In this context, aggregate size distribution encompasses both soil particles and aggregates, since they cannot be distinguished. The aggregate size distributions of Hamra and Loess soils (control), obtained from micro-CT images, showed a relatively narrow distribution in comparison to the distribution of Vertisol with prevalent aggregate sizes of 140, 75 and ~ 230 µm, respectively. The control distributions of Hamra and Loess suit their expected texture (Table 1) while for Vertisol, since the clay fraction is well aggregated, broad distribution is registered.

Following mucilage addition to the soils, a pronounced shift towards larger aggregates was obtained for Loess, indicating soil aggregation, while, for Hamra and Vertisol soils, the shifts were not noticeable. However, upon subtracting the distributions (mucilage minus the control; Fig. S2) a relatively small positive area (0.27) was obtained, even for the almost structureless Hamra sandy soil, for aggregates larger than 145 µm. In the difference distribution curve, the positive area indicates a gain in aggregate fractions of certain sizes, indicating moderate aggregation. As expected, the positive area, for aggregates larger than 110 µm, obtained for Loess was high (2.7) and the positive area obtained for Vertisol was negligible.

The dramatic enhanced Loess aggregation, following mucilage treatment, can be explained by the typical initial high quantity of small particles and aggregates (smaller than 110 µm) (Crouvi et al., 2008), which are prone to mucilage-induced aggregation. Likewise, the mild effect of mucilage on Hamra may be attributed to the medium quantity of small particles and aggregates (smaller than 145 µm) (Fig 2A). Despite the high clay content of Vertisol, 60% clay, the initial quantity of small aggregates (smaller than 110-145 µm) is very low, since the soil is highly aggregated, and therefore the contribution of mucilage is negligible. Similarly, studies conducted on soils with comparable origins have reported minimal increase aggregate stability in clay soils (>40% clay) as the clay content increased (Kharitonova et al., 2020; Norton et al., 2006).

https://doi.org/10.5194/egusphere-2023-2501
Preprint. Discussion started: 10 November 2023

These observations indicate that the degree of aggregation inversely correlates with the weighted percentage of large soil aggregates (250-2000 µm; 48, 30 and 15% for Vertisol, Hamra and Loess, respectively), which are most likely not aggregated by mucilage (Table S1).

To further characterize the involvement of the smaller aggregates (<100 µm) in the effect of mucilage on soil aggregation, we developed a new method based on SEM images (see section 2.5.2), with higher resolution, and clearer aggregate separation. Indeed, relatively narrow distributions were obtained at the smaller aggregate sizes with prevalent aggregate sizes of 50, 15 and 18 µm, for Hamra, Loess and Vertisol, respectively. In the presence of mucilage, the most pronounced aggregation (0.023- expressed as the positive area upon subtracting the distributions (Figure S2)) was observed for Hamra aggregates smaller than 100 µm which are 5.4% of the soil (w/w). Noticeable aggregation was also obtained for Loess (0.018) but for aggregates smaller than 50 µm which are ~12% (w/w). Also, in the case of Vertisol, aggregates smaller than 50 µm which are ~7% (w/w), were aggregated (0.009).

Obviously, the degree of aggregation is affected not only by the percentage of small aggregates, but also by their mineralogy. Lower degree of aggregation in the case of Vertisol was further explored by characterizing the mineralogy of the different soils. The clay fraction of Vertisol was dominated by swelling smectites while Hamra and Loess contained more illite and kaolinite (Table 2b). The small particles which are overlooked in the case of the CT results are registered by the SEM images that bring forward the aggregation processes of these small particles and emphasize the importance of quantifying the smaller soil particles and aggregates to fully understand the effect of mucilage on soil aggregation.

3.2 Effect of mucilage on soil stability

Soil stability measurements, assessed by aggregate durability index (ADI) and mean weight diameter (MWD) (measured following wet sieving) varied between the soils (Fig. 3a, S1). The average MWD values for Loess and Vertisol (control samples) were 0.08 and 0.33 mm, respectively, reflecting their texture and following the same tread as previous studies reporting a positive correlation between aggregate stability and clay content (Amézketa, 2008b). In addition, the MWD values increased significantly following mucilage treatment (measured after 7 days), where the relative increases in the stability of Loess and Vertisol were in the same trend as obtained in the ADI results. Despite the frequent use of the wet sieving stability index, it is tedious method and not suitable for sandy soils such as Hamra (high percentage of primary soil particles). We developed an advanced stability index (Dor et al., 2019), ADI, based on laser granulometry which can be used for sandy soils and is based on a continuous aggregate size distribution range, unlike the wet sieving (limited to the number and size of the sieves). The ADI values for Hamra, Loess and Vertisol (control samples) were 0.003, 0.056 and 0.4, respectively, reflecting their texture as well. The distinction between the soils ADI values was an order of magnitude higher, highlighting the sensitivity of the ADI for soil stability.

As we hypothesized, mucilage treatment not only brings upon aggregation but also significantly increased soil stability for all three soils ($p<0.05$), where the relative increases in the stability of Hamra, Loess and Vertisol were ~33%, ~68% and ~15%, respectively. The increase in stability indicates that mucilage not only acts as a glue, which binds the soil particles

https://doi.org/10.5194/egusphere-2023-2501
Preprint. Discussion started: 10 November 2023

together, but also creates stronger interactions between the particles resulting in enhanced soil stability. Previous studies have also shown that root mucilage collected from maize plants (*Zea mays L.*) increased soil aggregate stability immediately after the incorporation of mucilage into the soil, however, the concentration of mucilage was higher than the environmental concentration in the rhizosphere (was an order of magnitude) (Watt et al., 1993; Morel et al., 1991).

The degree of increase in soil stability is in agreement with the degree of aggregation (obtained from the CT) i.e., in the order of Loess, Hamra and Vertisol. As suggested, the highest degree of aggregation reported for Loess, was due to the initial high quantity of small particles and aggregates (smaller than 110 µm), which are prone to aggregate by mucilage.

To test whether these small particles also play a major role in soil stability, we measured the stability, pre and post mucilage treatment, of four soil aggregate size fractions <50, 50-100, 100-250 and 250-2000 µm (Fig. 4). Indeed, for the Loess and Hamra soils, the main size fractions contributing to stability were 100 µm, whereas for the Vertisol, the increase in stability was spread across all size fractions.

Interestingly, and strengthening the applicability and reliability of the developed aggregation durability index (ADI), the total soil ADI of the control and mucilage treatments (Fig. 4) were in agreement with the weighted ADI of the four size fractions (R^2=0.991 (Fig 3b)). These results suggest that soil texture, and specifically soil mineralogy are crucial factors that influence soil stability from the bottom up.

In order to address the variation of ADI with aggregate size distributions of the three different soils it is necessary to better understand the specific minerology of each soil (Table 2a). Based on the pedological soil survey of the three soil types (Singer, 2007) the aggregate size fraction smaller than 50 µm contains mostly clay minerals, where the 50-100 µm fraction highly contains silt, calcite and feldspar. The fraction larger than 100 µm contains quartz in the case of Hamra, while in the case of the Loess and Vertisol soils it contains mostly clay aggregates.

Accordingly, the ADI values of the <100 µm fractions of the Hamra soil were higher than the >100 µm fractions (Fig. 4a) reflecting the higher stability of clay-mineral aggregates compared to quartz. The ADI values of the <100 µm fractions of the Hamra were similar to their corresponding fractions of Loess soil. To further characterize the mineralogy of these soils, the fine fraction (<2 µm) was analysis by XRD (Table 2b). Indeed, both Hamra and Loess have similar percentage (~30%) of illite-smectite minerals, which considerably contribute to aggregate stability (Reid-Soukup and Ulery, 2018). However, the fractions larger than 100 µm showed higher values for the loess due to the high calcite content which is known to cement and stabilize Loess soil (Hochman et al., 2020)Table 2a).

In case of the Vertisol the percent of illite-smectite in the clay fraction is extremely high, ~70%, (Table 1,2) explaining the high ADI values across all size fractions. These minerals bring upon Vertisol aggregation, i.e., the small clay-mineral aggregates, with time, form larger and more stable structures and therefore an increase of ADI with aggregate size is observed.

Adding mucilage to the soils significantly increased the ADI values of the <50 and 50-100 µm fractions of Hamra and Loess soils, where in the 100-250 fraction, the increase of the ADI values was significant only for the Loess soil. In the case of Vertisol, the increases in the ADI values were not significant. These results strengthen our conclusion that mucilage mainly

https://doi.org/10.5194/egusphere-2023-2501
Preprint. Discussion started: 10 November 2023

stabilizes the <250 μm fraction in soils, therefore the total effect of mucilage on soil stability may depend on the soil aggregates size distribution.

To better demonstrate the contribution of each aggregate size faction to the total increase in soil stability, we calculated a 'weighted stability growth' i.e., we multiplied the degree of stability increase by the weight of the faction (w/w) (Figure 4d). High values of the 'weighted stability growth', correspond to a larger stability contribution for the specific size fraction.

The highest value obtained was for the 50-100 μm fraction of the Loess which is in line with the highest increase (68%) in the total ADI of this soil (Fig. 3a). The micro-CT results also showed that particles and aggregates smaller than ~100 μm are the main participants in Loess aggregation. In the case of Hamra (with a total soil stability increase of 33%), the micro-CT results showed that larger aggregates participate and indeed a high 'weighted stability growth' value was obtained for Hamra aggregates of 100-250 μm. Consistently the stability of Vertisol was only slightly affected by mucilage.

These findings emphasize the significance of the size fraction and the clay-minerals as key factors in maintaining aggregate stability as demonstrated in the stability of the two contrasting soils, the sandy Hamra and the clayey vertisol. In vertisol, clay-minerals are distributed throughout all size fractions, serving as the building units of microaggregates (Totsche et al., 2018). In contrast, due to the high percentage of sand, in Hamra clay-minerals are primarily present in the finer fraction, where the most substantial improvement in aggregate stability was measured. Moreover, upon examining the interplay between the two aforementioned factors, size fraction and mineralogy, in conjunction with mucilage addition, the most pronounced contribution to soil stability occurs in the finer size fraction of the Hamra, which is where the largest proportion of surface area is available for binding.

3.3 Effect of in-situ root exudates on soil stability

Finally, to test the *in-situ* effect of root exudates on Hamra, Loess and Vertisol stability the ADI values of the soils were measured after growing Chia plants in the different soils for 14 days (Fig. 5). The significant increases in ADI values for Hamra and Loess reached 29% and 96% ($p=0.0051$), respectively, where the none-significant increase in Vertisol reached 0.1% ($p=0.487$). These trends very well correlate with the trends obtained upon the artificial addition of mucilage after 7 days (Fig. 5a).

3.4 The effect of WDC on the contribution of mucilage on soil packing and stability

While the biochemical driver, mucilage, induces aggregation for all three soils tested, the physical driver, wetting and drying cycle (WDC) induced diverse trends; aggregation, disaggregation on Loess and Vertisol, respectively (Hochman et al., 2020). As expected, the ADI of the Hamra did not change significantly after WDC, due to its lack of structure.

We explored whether soils subjected to mucilage, followed by WDC, would further enhance aggregation or may even overcome disaggregation, in the case of Loess and Vertisol, respectively. The change in the packing and stability of Loess and Vertisol soils subjected and not subjected to mucilage, followed by WDC, were characterized by micro-CT and ADI measurements (Fig. 6).

https://doi.org/10.5194/egusphere-2023-2501
Preprint. Discussion started: 10 November 2023

As previously reported (Hochman et al., 2020), upon subjecting Loess to a WDC, aggregate size distribution shifted towards larger aggregates (Fig. 6a) and accordingly stability increased (~27%) (Fig. 6c) which was explain by aggregate cementation in calcite-rich soils (such as Loess). As hypothesized, for Loess subjected to mucilage, followed by a WDC, aggregation was intensified as shown by an increase in aggregate size distribution and by an increase in ADI (~98%, ~56% and ~17% from control, post WDC and mucilage, respectively). On the other hand, upon subjecting Vertisol to a WDC, aggregate size distribution shifted towards smaller aggregates (Fig. 6b) and accordingly stability significantly decreased (~47%) (Fig. 6d), reflecting disaggregation of clayey soils.

For Vertisol subjected to mucilage, followed by a WDC, disaggregation was not obtained, but rather an increase in aggregate size distribution and a significant increase in ADI were measured (~51% increase in ADI values) (Fig. 6d) indicating aggregation. These results emphasize that adding mucilage to Loess and Vertisol, intensified and overcame, the aggregation and disaggregation induced by WDC, respectively.

Mucilage is known to promote a hysteretic behavior of soil water retention during WDC, resulting in higher water content in the rhizosphere than in the bulk soil during the drying period, followed by a lower rate rehydration of the rhizosphere than the bulk soil (Ahmed et al., 2014; Ali Ahmed et al., 2016; Carminati et al., 2010; Paporisch et al., 2021), which can moderate the effect of WDC on soil structure.

3.5 The dynamic effect of mucilage and microorganisms on soil stability

While the biochemical driver, mucilage, induces aggregation, the physical driver, wetting and drying cycle (WDC) induced aggregation or disaggregation. Soil biological drivers, the most dynamic, intricate and unknow, add complexity. For example, the consumption of mucilage by soil microorganisms may promote two opposing processes in terms of soil stability. On one hand, the root mucilage is an energy source for microorganisms that produce a variety of extracellular polymeric substances (EPS) which in turn contribute to aggregate formation and stabilization. On the other hand, consuming the root mucilage may weaken soil structure.

To explore the dynamic effects of mucilage on soil microorganism activity and soil stability, the cumulative soil respiration (for 7 days) and ADI values (monitored with time for 7 days) were measured, respectively (Fig 7).

The obtained respiration values of the Vertisol were higher than those of Loess (1.66 and 0.67 mg/gr soil, respectively) even upon normalizing to organic C (%) which served as proxy for the total organic matter and microbial biomass. Since Vertisol has a higher clay content, it retains more water and provides a favorable habitat for microorganisms (Brockett et al., 2012). Additionally, these trends were also obtained in the work of Nazari et al. (2022) and were explained by the higher availability of the organic matter and nutrient content in the Vertisol, which is known to stimulate microbial population size and activity. As expected, following mucilage addition, soil respiration, for Vertisol and Loess soils increased significantly within week ($p<0.05$) by 20% and 15%, respectively, indicating mucilage consumption by the microorganisms. The observed high respiration was previously related to the chemical composition and high solubility of mucilage, which stimulates microbial activity in its vicinity, leading to this priming effect (Kuzyakov, 2010; Kuzyakov et al., 2000) which in turn contributes to soil aggregation and stability (Baumert et al., 2018). Indeed, as reported above, within a week, ADI values also increase upon the addition of mucilage. However, to better understand the dynamic and mutual effects on of these two parameters, mucilage and microorganism, on soil stability ADI values were monitored with time.

ADI values of Vertisol and Loess, control and mucilage treatments, decreased and increased within three days, respectively, and then remained constant. The decrease and increase within three days reflect disaggregation and aggregation processes induced by Vertisol and Loess drying, respectively, as previously explained (fig 6). A steady state was reached within three days with significant ($p<0.05$) higher ADI values for the mucilage treated soils. Morel et al. (1991) have shown that the presence of maize root mucilage in soil generated a lag phase of 48 hours (the delay before the start of bacteria exponential growth) (Morel et al., 1991), which can explain the delayed effect of mucilage on soil stability in our results.

The observed steady state in the ADI values could be explained by compensating microorganism activities i.e., root mucilage consumption and self-extracellular polymeric substances production. Such substances play important roles in the formation and persistence of microbial biofilms in soils, which are also facilitate soil aggregation (Costa et al., 2018). According to Nazari et al., (2022) EPS and plant mucilage share an overall high degree of similarity in the physical and chemical properties, suggesting that plant mucilage can function as a biofilm matrix similar to EPS, covering a large extent of the rhizosphere (Nazari et al., 2022). Clearly, studies on the intricate and dynamic effect of mucilage and soil microorganisms on soil structure are scarce and should be further investigated.

4 Conclusions

This study contributes to a better understanding of the rhizosphere structure, which is primarily shaped by root exudates and microbial activity. It provides an innovative and efficient approach to integrate advanced imaging methods with quantification of soil structural changes. We quantified the effect of mucilage, a biochemical driver, on soil structure parameters, packing and stability, in three soils, measured and analyzed by micro-CT, SEM and laser granulometry methods. To the best of our knowledge for the first time, we were able to visualize the binding of soil particles by mucilage at environmental concentrations. For the three studied soils, mucilage increased soil aggregate sizes (i.e., aggregation) coupled with aggregate stability enhancement. However, the intensity of these enhancements varied between the soils, in the order of Loess > Hamra > Vertisol. The trend was also obtained *in-situ*, when chia seeds were sown and grown in the soils. Our results show a clear correlation between the aggregate size distribution of the soil and the effect of mucilage on soil stability where small soil aggregates (<250 um) have the largest role in aggregation and stabilization processes.

To increase the complexity of the study, we investigated the coupled effects of the biochemical driver, mucilage, and a physical driver, wetting and drying, on soil stability and packing. We found that adding mucilage to Loess and Vertisol intensified and overcame the aggregation and disaggregation induced by WDC, respectively, verified by micro-CT and ADI measurements.

Mucilage increases soil stability and packing but also triggers many dynamic soil processes such as soil microorganism activity, as measured by CO_2 respiration. To better understand the dynamic and mutual effects of these two parameters, mucilage and microorganism, on soil stability ADI values were monitored with time. A steady state was reached within three days with significantly higher ADI values for the mucilage treated soils. This steady state could be explained by compensating microorganism activities, root mucilage consumption and self-mucilaginous polysaccharides production.

The results of this study provide quantitative and conceptual insight into the effects of mucilage on soil packing and stability over a range of scales. The outcome of this study presents a new approach to integrate advanced imaging methods with quantification of soil structural changes. The results, demonstrate the intricate and dynamic effect of mucilage on soil structure and will undoubtedly inspire future studies aimed at exploring how soil structural dynamics influence soil functions, such as carbon and water storage, nutrient cycling, microbial habitat, and physical stability, and thereby offer strategies for better soil erosion management.

5 References

Ahmed, M. A., Kroener, E., Holz, M., Zarebanadkouki, M., and Carminati, A.: Mucilage exudation facilitates root water uptake in dry soils, in: Functional Plant Biology, 1129–1137, https://doi.org/10.1071/FP13330, 2014.

Ali Ahmed, M., Kroener, E., Benard, P., Zarebanadkouki, M., Kaestner, A., Carminati, A., Ahmed, M. A., Kroener, E., Benard, P., Zarebanadkouki, M., Carminati, A., and Kaestner, A.: Drying of mucilage causes water repellency in the rhizosphere of maize: measurements and modelling, Plant Soil, 407, 161–171, https://doi.org/10.1007/s11104-015-2749-1, 2016.

Alletto, L., Coquet, Y., Benoit, P., Heddadj, D., and Barriuso, E.: Tillage management effects on pesticide fate in soils. A review, Agronomy for Sustainable Development 2009 30:2, 30, 367–400, https://doi.org/10.1051/AGRO/2009018, 2012.

Amézketa, E.: Soil Aggregate Stability: A Review, Journal of sustainable agriculture, 14, 83–151, https://doi.org/10.1300/J064V14N02_08, 2008a.

Amézketa, E.: Soil Aggregate Stability: A Review, http://dx.doi.org/10.1300/J064v14n02_08, 14, 83–151, https://doi.org/10.1300/J064V14N02_08, 2008b.

Assouline, S. and Mualem, Y.: Modeling the dynamics of seal formation and its effect on infiltration as related to soil and rainfall characteristics, Water Resources Research, 33, 1527–1536, https://doi.org/10.1029/96WR02674, 1997.

Ball, B. C.: Soil structure and greenhouse gas emissions: a synthesis of 20 years of experimentation, European Journal of Soil Science, 64, 357–373, https://doi.org/10.1111/ejss.12013, 2013.

Bartha, R. and Parmer, D.: Features of a Flask and Method for Measuring the Persistence and Biological Effects of Pesticides in Soil, Soil Science, 100, 1965.

Barthès, B. and Roose, E.: Aggregate stability as an indicator of soil susceptibility to runoff and erosion; validation at several levels, CATENA, 47, 133–149, https://doi.org/10.1016/S0341-8162(01)00180-1, 2002.

Baumert, V. L., Vasilyeva, N. A., Vladimirov, A. A., Meier, I. C., Kögel-Knabner, I., and Mueller, C. W.: Root Exudates Induce Soil Macroaggregation Facilitated by Fungi in Subsoil, Frontiers in Environmental Science, 6, 2018.

Bavel, C. H. M. van: Mean Weight-Diameter of Soil Aggregates as a Statistical Index of Aggregation, Soil Science Society of America Journal, 14, 20–23, https://doi.org/10.2136/SSSAJ1950.036159950014000C0005X, 1950.

Baveye, P. C., Balseiro-Romero, M., Bottinelli, N., Briones, M., Capowiez, Y., Garnier, P., Kravchenko, A., Otten, W., Pot, V., SchluÌˆter, S., Vogel, H.-J., Baveye, P. C., Balseiro-Romero, M., Bottinelli, N., Briones, M., Capowiez, Y., Garnier, P., Kravchenko, A., Otten, W., Pot, V., SchluÌˆter, S., and Vogel, H.-J.: Lessons from a landmark 1991 article on soil structure: distinct precedence of non-destructive assessment and benefits of fresh perspectives in soil research, Soil Res., 60, 321–336, https://doi.org/10.1071/SR21268, 2022.

Berg, S., Kutra, D., Kroeger, T., Straehle, C. N., Kausler, B. X., Haubold, C., Schiegg, M., Ales, J., Beier, T., Rudy, M., Eren, K., Cervantes, J. I., Xu, B., Beuttenmueller, F., Wolny, A., Zhang, C., Koethe, U., Hamprecht, F. A., and Kreshuk, A.: ilastik: interactive machine learning for (bio)image analysis, Nature Methods, https://doi.org/10.1038/s41592-019-0582-9, 2019.

Biscaye, P. E.: Mineralogy and Sedimentation of Recent Deep-Sea Clay in the Atlantic Ocean and Adjacent Seas and Oceans, GSA Bulletin, 76, 803–832, https://doi.org/10.1130/0016-7606(1965)76[803:MASORD]2.0.CO;2, 1965.

Le Bissonnais, Y., Prieto, I., Roumet, C., Nespoulous, J., Metayer, J., Huon, S., Villatoro, M., and Stokes, A.: Soil aggregate stability in Mediterranean and tropical agro-ecosystems: effect of plant roots and soil characteristics, Plant and Soil, 424, 303–317, https://doi.org/10.1007/S11104-017-3423-6/FIGURES/3, 2018.

Brockett, B. F. T., Prescott, C. E., and Grayston, S. J.: Soil moisture is the major factor influencing microbial community structure and enzyme activities across seven biogeoclimatic zones in western Canada, Soil Biology and Biochemistry, 44, 9–20, https://doi.org/10.1016/J.SOILBIO.2011.09.003, 2012.

Bronick, C. J. and Lal, R.: Soil structure and management: a review, Geoderma, 124, 3–22, https://doi.org/10.1016/J.GEODERMA.2004.03.005, 2005.

Cantón, Y., Solé-Benet, A., Asensio, C., Chamizo, S., and Puigdefábregas, J.: Aggregate stability in range sandy loam soils Relationships with runoff and erosion, CATENA, 77, 192–199, https://doi.org/10.1016/j.catena.2008.12.011, 2009.

Capitani, M. I., Ixtaina, V. Y., Nolasco, S. M., and Tomás, M. C.: Microstructure, chemical composition and mucilage exudation of chia (Salvia hispanica L.) nutlets from Argentina, Journal of the Science of Food and Agriculture, 93, 3856–3862, https://doi.org/10.1002/jsfa.6327, 2013.

Carminati, A. and Vetterlein, D.: Plasticity of rhizosphere hydraulic properties as a key for efficient utilization of scarce resources, Annals of Botany, 112, 277–290, https://doi.org/10.1093/AOB/MCS262, 2013.

Carminati, A., Moradi, A. B., Vetterlein, D., Vontobel, P., Lehmann, E., Weller, U., Vogel, H.-J., and Oswald, S. E.: Dynamics of soil water content in the rhizosphere, Plant and Soil 2010 332:1, 332, 163–176, https://doi.org/10.1007/S11104-010-0283-8, 2010.

Cerdà, A.: Soil aggregate stability under different Mediterranean vegetation types, CATENA, 32, 73–86, https://doi.org/10.1016/S0341-8162(98)00041-1, 1998.

Chaboud, A.: Isolation, purification and chemical composition of maize root cap slime, Plant and Soil, 73, 395–402, https://doi.org/10.1007/BF02184316, 1983.

Chaboud, A. and Rougier, M.: Identification and Localization of Sugar Components of Rice (Oryza sativa L.) Root Cap Mucilage, Journal of Plant Physiology, 116, 323–330, https://doi.org/10.1016/S0176-1617(84)80111-X, 1984.

Chipera, S. J. and Bish, D. L.: FULLPAT: a full-pattern quantitative analysis program for X-ray powder diffraction using measured and calculated patterns, Journal of Applied Crystallography, 35, 744–749, https://doi.org/10.1107/S0021889802017405, 2002.

Christensen, B. T.: Physical fractionation of soil and structural and functional complexity in organic matter turnover, European Journal of Soil Science, 52, 345–353, https://doi.org/10.1046/j.1365-2389.2001.00417.x, 2001.

Costa, O. Y. A., Raaijmakers, J. M., and Kuramae, E. E.: Microbial extracellular polymeric substances: Ecological function and impact on soil aggregation, Frontiers in Microbiology, 9, 1636, https://doi.org/10.3389/FMICB.2018.01636/BIBTEX, 2018.

Crouvi, O., Amit, R., Enzel, Y., Porat, N., and Sandler, A.: Sand dunes as a major proximal dust source for late Pleistocene loess in the Negev Desert, Israel, Quaternary Research, 70, 275–282, https://doi.org/10.1016/j.yqres.2008.04.011, 2008.

Czarnes, S., Hallett, P. D., Bengough, A. G., and Young, I. M.: Influence de mucilages racinaire et microbiens modeles sur la structure du sol et le transport d'eau, European Journal of Soil Science, 51, 435–443, https://doi.org/10.1046/J.1365-2389.2000.00327.X, 2000.

Dor, M., Emmanuel, S., Brumfeld, V., Levy, G. J., and Mishael, Y. G.: Microstructural changes in soils induced by wetting and drying: Effects on atrazine mobility, Land Degradation and Development, 30, 746–755, https://doi.org/10.1002/ldr.3256, 2019.

Doube, M., Klosowski, M. M., Arganda-Carreras, I., Cordelières, F. P., Dougherty, R. P., Jackson, J. S., Schmid, B., Hutchinson, J. R., and Shefelbine, S. J.: BoneJ: Free and extensible bone image analysis in ImageJ, Bone, 47, 1076–1079, https://doi.org/10.1016/J.BONE.2010.08.023, 2010.

Gao, Z., Bian, L., Hu, Y., Wang, L., and Fan, J.: Determination of soil temperature in an arid region, Journal of Arid Environments, 71, 157–168, https://doi.org/10.1016/j.jaridenv.2007.03.012, 2007.

Gee, G. W. and Or, D.: 2.4 Particle-Size Analysis, in: Methods of Soil Analysis, John Wiley & Sons, Ltd, 255–293, https://doi.org/10.2136/sssabookser5.4.c12, 2002.

Hadas, A. and Stibbe, E.: Soil Crusting and Emergence of Wheat Seedlings 1, Agronomy Journal, 69, 547–550, https://doi.org/10.2134/agronj1977.00021962006900040006x, 1977.

Hochman, D., Dor, M., and Mishael, Y.: Diverse Effects of Wetting and Drying Cycles on Soil Aggregation: Implications on Pesticide Leaching, Chemosphere, 263, 127910, https://doi.org/10.1016/j.chemosphere.2020.127910, 2020.

Holz, M., Leue, M., Ahmed, M. A., Benard, P., Gerke, H. H., and Carminati, A.: Spatial distribution of mucilage in the rhizosphere measured with infrared spectroscopy, Frontiers in Environmental Science, 6, 87, https://doi.org/10.3389/fenvs.2018.00087, 2018.

Kharitonova, G. V., Kot, F. S., and Krutikova, V. O.: Carbonate and concomitant microaggregation in irrigated Mediterranean soils of Israel, Irrig Sci, 38, 431–447, https://doi.org/10.1007/s00271-020-00685-0, 2020.

Koestel, J.: SoilJ: An ImageJ Plugin for the Semiautomatic Processing of Three-Dimensional X-ray Images of Soils, Vadose Zone Journal, 17, 170062, https://doi.org/10.2136/vzj2017.03.0062, 2018.

Kroener, E., Zarebanadkouki, M., Kaestner, A., and Carminati, A.: Nonequilibrium water dynamics in the rhizosphere: How mucilage affects water flow in soils, Water Resources Research, 50, 6479–6495, https://doi.org/10.1002/2013WR014756, 2014.

Lal, R.: Soil degradation by erosion, Land Degradation & Development, 12, 519–539, https://doi.org/10.1002/LDR.472, 2001.

Levy, G. J. and Mamedov, A. I.: High-Energy-Moisture-Characteristic Aggregate Stability as a Predictor for Seal Formation, Soil Science Society of America Journal, 66, 1603–1609, https://doi.org/10.2136/sssaj2002.1603, 2002.

Loeppert, R. H. and Suarez, D. L.: Carbonate and Gypsum, in: Methods of Soil Analysis, John Wiley & Sons, Ltd, 437–474, https://doi.org/10.2136/sssabookser5.3.c15, 1996.

Moore, D. M. and Reynolds, R. C.: X-ray diffraction and the identification and analysis of clay minerals., X-ray diffraction and the identification and analysis of clay minerals., 1989.

Morel, J. L., Andreux, F., Habib, L., and Guckert, A.: Comparison of the adsorption of maize root mucilage and polygalacturonic acid on montmorillonite homoionic to divalent lead and cadmium, Biology and Fertility of Soils, 5, 13–17, https://doi.org/10.1007/BF00264339, 1987.

Morel, J. L., Habib, L., Plantureux, S., and Guckert, A.: Influence of maize root mucilage on soil aggregate stability, Plant and Soil 1991 136:1, 136, 111–119, https://doi.org/10.1007/BF02465226, 1991.

Nazari, M., Bickel, S., Benard, P., Mason-Jones, K., Carminati, A., and Dippold, M. A.: Biogels in Soils: Plant Mucilage as a Biofilm Matrix That Shapes the Rhizosphere Microbial Habitat, Frontiers in Plant Science, 12, https://doi.org/10.3389/fpls.2021.798992, 2022.

Nciizah, A. D. and Wakindiki, I. I. C.: Physical indicators of soil erosion, aggregate stability and erodibility, Archives of Agronomy and Soil Science, 61, 827–842, https://doi.org/10.1080/03650340.2014.956660, 2015.

Norton, L. D., Mamedov, A. I., Huang, C., and Levy, Guy J.: Soil Aggregate Stability as Affected by Long-Term Tillage and Clay Mineralogy, Soil aggregate stability as affected by long-term tillage and clay minerology, 38, 421–429, 2006.

Oades, J. M.: The role of biology in the formation, stabilization and degradation of soil structure, Geoderma, 56, 377–400, https://doi.org/10.1016/0016-7061(93)90123-3, 1993.

Or, D., Keller, T., and Schlesinger, W. H.: Natural and managed soil structure: On the fragile scaffolding for soil functioning, Soil and Tillage Research, 208, 104912, https://doi.org/10.1016/j.still.2020.104912, 2021.

Otsu, N.: THRESHOLD SELECTION METHOD FROM GRAY-LEVEL HISTOGRAMS., IEEE Trans Syst Man Cybern, SMC-9, 62–66, https://doi.org/10.1109/TSMC.1979.4310076, 1979.

Paporisch, A., Bavli, H., Strickman, R. J., Neumann, R. B., and Schwartz, N.: Root Exudates Alters Nutrient Transport in Soil, Water Resources Research, 57, https://doi.org/10.1029/2021WR029976, 2021.

Pardo, A., Amato, M., and Chiarandà, F. Q.: Relationships between soil structure, root distribution and water uptake of chickpea (Cicer arietinum L.). Plant growth and water distribution, European Journal of Agronomy, 13, 39–45, https://doi.org/10.1016/S1161-0301(00)00056-3, 2000.

Popović, Z. and Cerdà, A.: Soil water repellency and plant cover: A state-of-knowledge review, CATENA, 229, 107213, https://doi.org/10.1016/j.catena.2023.107213, 2023.

Potchter, O., Goldman, D., Kadish, D., and Iluz, D.: The oasis effect in an extremely hot and arid climate: The case of southern Israel, Journal of Arid Environments, 72, 1721–1733, https://doi.org/10.1016/j.jaridenv.2008.03.004, 2008.

Rabot, E., Wiesmeier, M., Schlüter, S., and Vogel, H.-J.: Soil structure as an indicator of soil functions: A review, Geoderma, 314, 122–137, https://doi.org/10.1016/j.geoderma.2017.11.009, 2018.

Reid-Soukup, D. A. and Ulery, A. L.: Smectites, Soil Mineralogy with Environmental Applications, 7, 467–499, https://doi.org/10.2136/SSSABOOKSER7.C15, 2018.

Schindelin, J., Arganda-Carreras, I., Frise, E., Kaynig, V., Longair, M., Pietzsch, T., Preibisch, S., Rueden, C., Saalfeld, S., Schmid, B., Tinevez, J. Y., White, D. J., Hartenstein, V., Eliceiri, K., Tomancak, P., and Cardona, A.: Fiji: an open-source platform for biological-image analysis, Nature Methods 2012 9:7, 9, 676–682, https://doi.org/10.1038/nmeth.2019, 2012.

Shukla, M. K., Lal, R., and Ebinger, M.: Determining soil quality indicators by factor analysis, Soil and Tillage Research, 87, 194–204, https://doi.org/10.1016/J.STILL.2005.03.011, 2006.

Singer, A.: The Soils of Israel The Soils of Israel, Springer, 2007.

Tisdall, J. M. and Oades, J. M.: Organic matter and water-stable aggregates in soils, Journal of Soil Science, 33, 141–163, https://doi.org/10.1111/j.1365-2389.1982.tb01755.x, 1982.

Totsche, K. U., Amelung, W., Gerzabek, M. H., Guggenberger, G., Klumpp, E., Knief, C., Lehndorff, E., Mikutta, R., Peth, S., Prechtel, A., Ray, N., and Kögel-Knabner, I.: Microaggregates in soils, Journal of Plant Nutrition and Soil Science, 181, 104–136, https://doi.org/10.1002/jpln.201600451, 2018.

Virtanen, P., Gommers, R., Oliphant, T. E., Haberland, M., Reddy, T., Cournapeau, D., Burovski, E., Peterson, P., Weckesser, W., Bright, J., van der Walt, S. J., Brett, M., Wilson, J., Millman, K. J., Mayorov, N., Nelson, A. R. J., Jones, E., Kern, R., Larson, E., Carey, C. J., Polat, İ., Feng, Y., Moore, E. W., VanderPlas, J., Laxalde, D., Perktold, J., Cimrman, R., Henriksen, I., Quintero, E. A., Harris, C. R., Archibald, A. M., Ribeiro, A. H., Pedregosa, F., van Mulbregt, P., Vijaykumar, A., Bardelli, A. Pietro, Rothberg, A., Hilboll, A., Kloeckner, A., Scopatz, A., Lee, A., Rokem, A., Woods, C. N., Fulton, C., Masson, C., Häggström, C., Fitzgerald, C., Nicholson, D. A., Hagen, D. R., Pasechnik, D. V., Olivetti, E., Martin, E., Wieser, E., Silva, F., Lenders, F., Wilhelm, F., Young, G., Price, G. A., Ingold, G. L., Allen, G. E., Lee, G. R., Audren, H., Probst, I., Dietrich, J. P., Silterra, J., Webber, J. T., Slavič, J., Nothman, J., Buchner, J., Kulick, J., Schönberger, J. L., de Miranda Cardoso, J. V., Reimer, J., Harrington, J., Rodríguez, J. L. C., Nunez-Iglesias, J., Kuczynski, J., Tritz, K., Thoma, M., Newville, M., Kümmerer, M., Bolingbroke, M., Tartre, M., Pak, M., Smith, N. J., Nowaczyk, N., Shebanov, N., Pavlyk, O., Brodtkorb, P. A., Lee, P., McGibbon, R. T., Feldbauer, R., Lewis, S., Tygier, S., Sievert, S., Vigna, S., Peterson, S., More, S., Pudlik, T., et al.: SciPy 1.0: fundamental algorithms for scientific computing in Python, Nature Methods 2020 17:3, 17, 261–272, https://doi.org/10.1038/s41592-019-0686-2, 2020.

Vogel, H.-J., Balseiro-Romero, M., Kravchenko, A., Otten, W., Pot, V., Schlüter, S., Weller, U., and Baveye, P. C.: A holistic perspective on soil architecture is needed as a key to soil functions, European Journal of Soil Science, 73, e13152, https://doi.org/10.1111/ejss.13152, 2022.

Walker, T. S., Bais, H. P., Grotewold, E., and Vivanco, J. M.: Root exudation and rhizosphere biology, https://doi.org/10.1104/pp.102.019661, 2003.

https://doi.org/10.5194/egusphere-2023-2501
Preprint. Discussion started: 10 November 2023

Watt, M., McCully, M. E., and Jeffree, C. E.: Plant and bacterial mucilages of the maize rhizosphere: Comparison of their soil binding properties and histochemistry in a model system, Plant and Soil, 151, 151–165, https://doi.org/10.1007/BF00016280, 1993.

Young, I. M. and Crawford, J. W.: Interactions and self-organization in the soil-microbe complex, https://doi.org/10.1126/science.1097394, 11 June 2004.

Yudina, A. and Kuzyakov, Y.: Dual nature of soil structure: The unity of aggregates and pores, Geoderma, 434, 116478, https://doi.org/10.1016/j.geoderma.2023.116478, 2023.

Zickenrott, I. M., Woche, S. K., Bachmann, J., Ahmed, M. A., and Vetterlein, D.: An efficient method for the collection of root mucilage from different plant species—A case study on the effect of mucilage on soil water repellency, Journal of Plant Nutrition and Soil Science, 179, 294–302, https://doi.org/10.1002/jpln.201500511, 2016.

Table 1: Soil Properties

Soil	Site	Texture	Sand (%)	Silt (%)	Clay (%)	OM (%)	$CaCO_3$ (%)
Hamra	Rehovot	Loamy sand	87.5	2.5	10	1.9	0.9
Loess	Mishmar-Hanegev	Sandy- clay-loam	60.5	17.5	21.9	2.9	19.5
Vertisol	Ein Harod	Clay	25	15	60	3.5	7.9

https://doi.org/10.5194/egusphere-2023-2501
Preprint. Discussion started: 10 November 2023

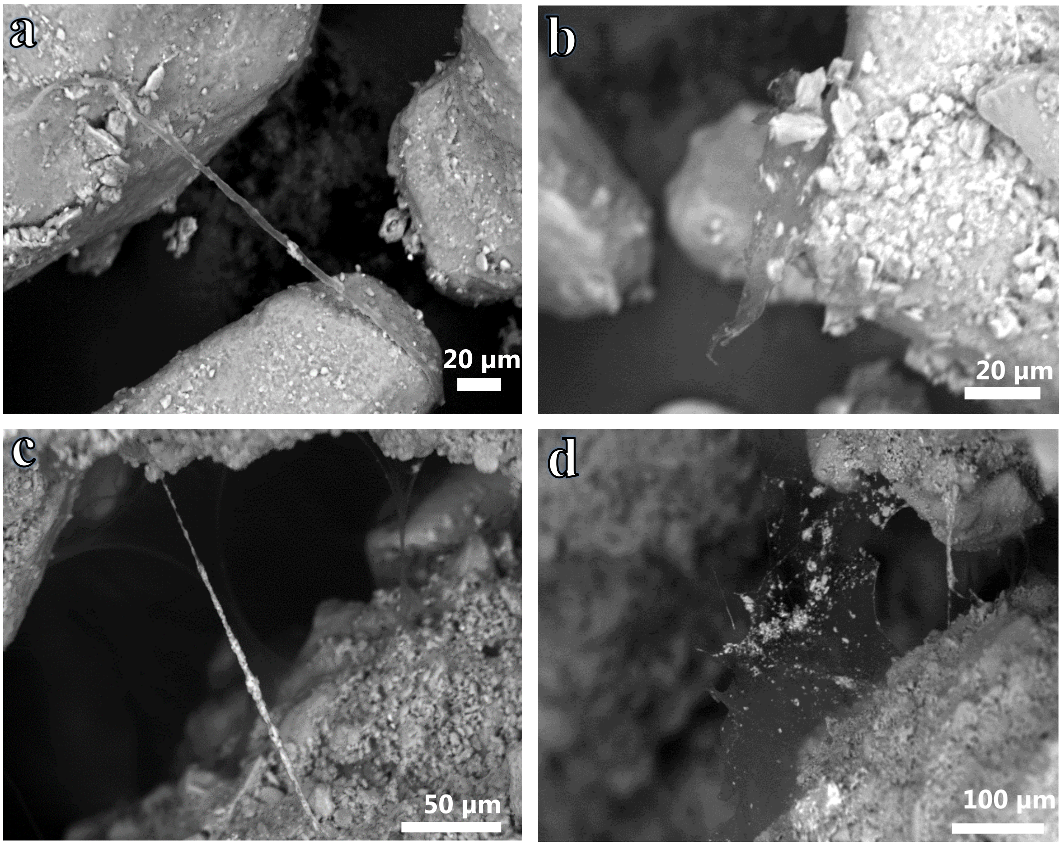

Figure 1 – Mucilage in Hamra (a,b) and Loess (c,d) soils (0.035% w/w) imaged with scanning electron microscope. The images highlight two binding configurations: strings (a,c) and webs (b, d).

https://doi.org/10.5194/egusphere-2023-2501
Preprint. Discussion started: 10 November 2023

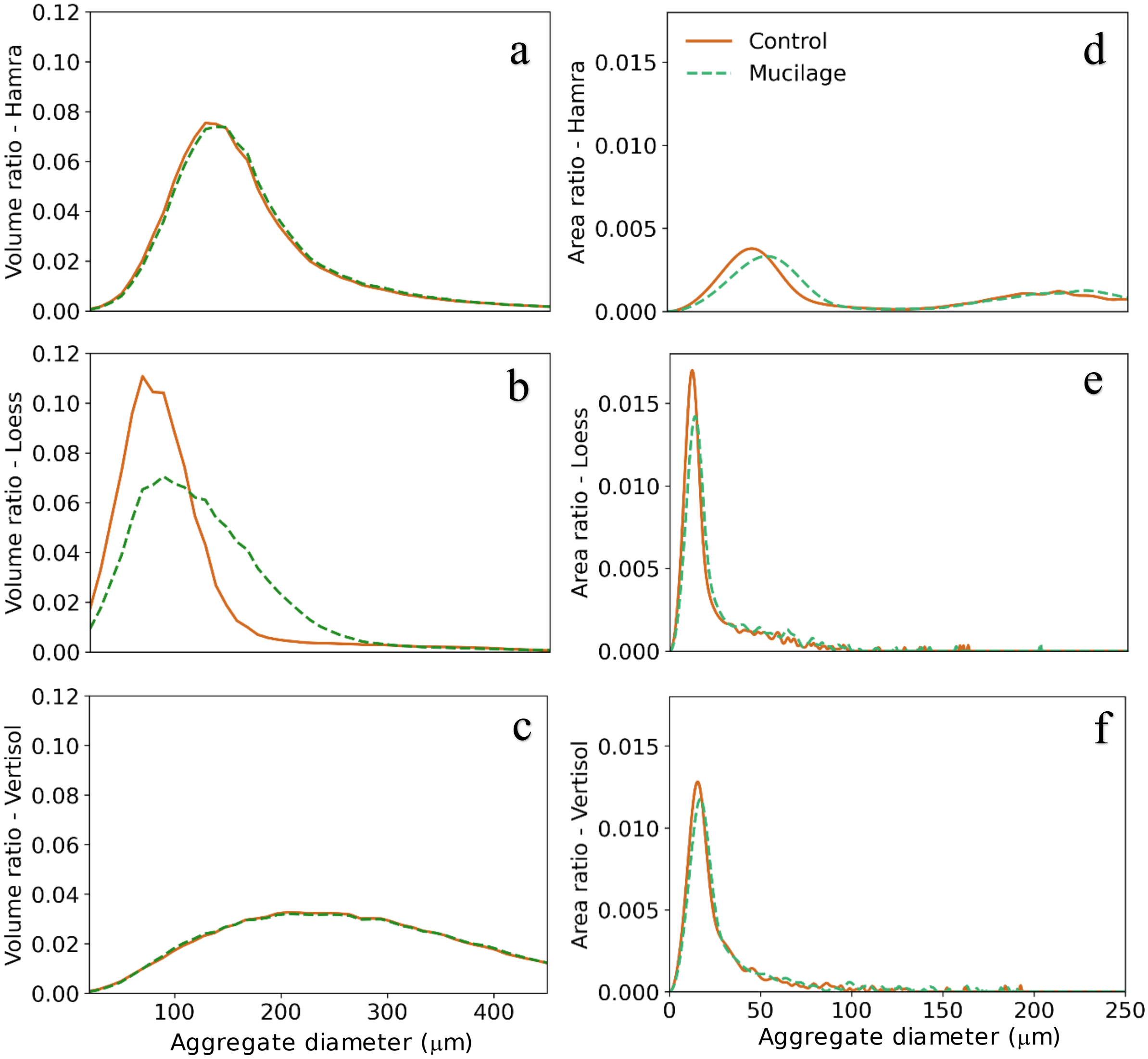

Figure 2: Aggregate size (diameter) distributions of the soils pre and post mucilage addition, (a-c) derived from micro-CT measurements and presented as volume ratios and (d-f) derived from SEM images presented as area ratios.

https://doi.org/10.5194/egusphere-2023-2501
Preprint. Discussion started: 10 November 2023

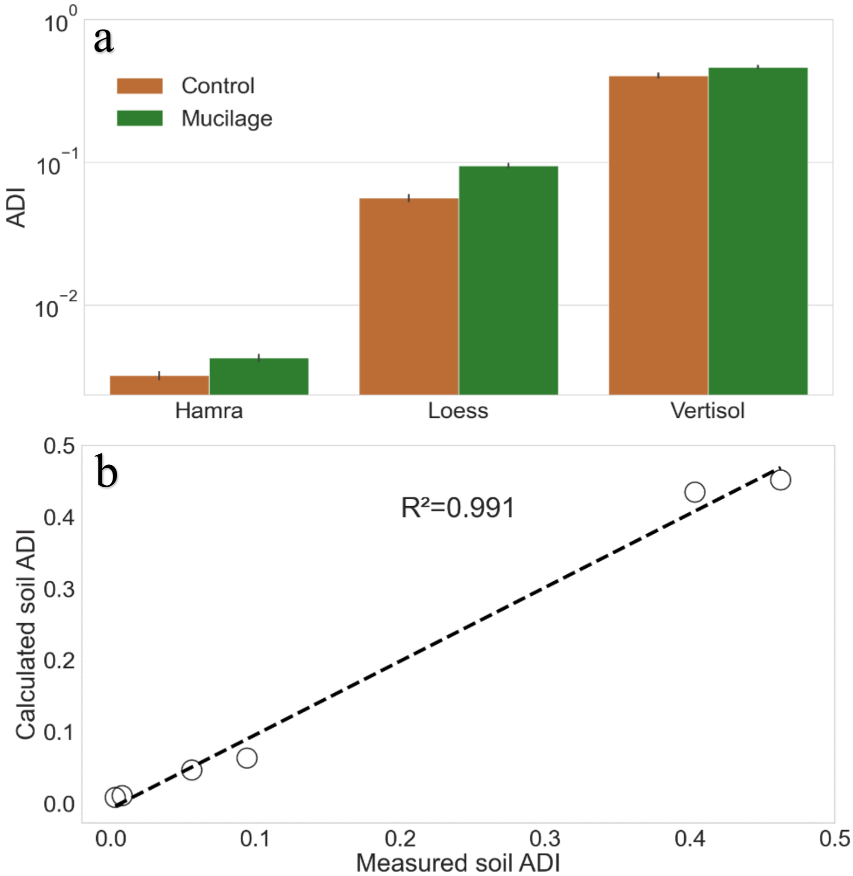

Figure 3: (a) ADI values of the soils pre and post mucilage addition and (b) ADI measured for bulk soils versus calculated for weighted size fractionated soils.

https://doi.org/10.5194/egusphere-2023-2501
Preprint. Discussion started: 10 November 2023

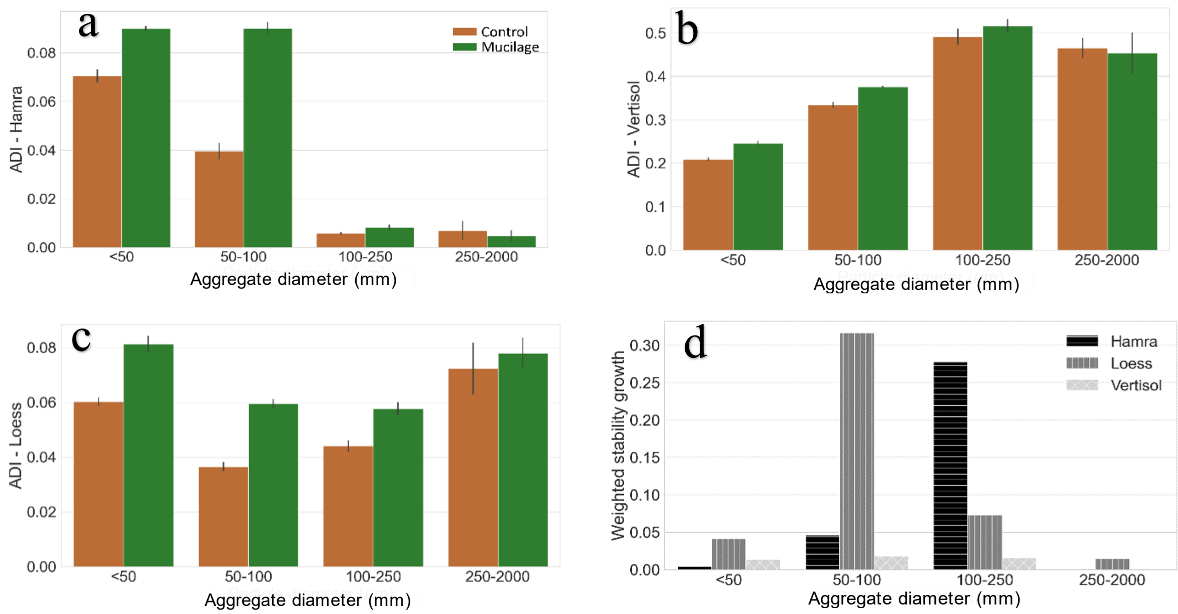

Figure 4: ADI values for aggregate size fractionation for (a) Hamra (b) Loess (c) Vertisol. (d) Weighted stability increase by size fraction, showing the proportion of different sizes contributing the total increase in stability.

570

https://doi.org/10.5194/egusphere-2023-2501
Preprint. Discussion started: 10 November 2023

Table 2 – Mineralogical composition. (a) Bulk soil mineralogical composition (%); (b) mineralogical composition of oriented clay fraction (<2 µm). Abbreviations according to order of appearance: I/S- Illite-smectite, P- Palygorskite, I- Illite, K- Kaolinite, Chl – Chlorite.

a)

Soil	Quartz	Plagioclase	K-Feldspar	Calcite	Dolomite	Goethite	Phyllosilicates	Amorphous
Hamra	41.5	3.9	7.5	10.7	6.8	3.2	12.7	13.8
Loess	20.4	2.3	4.8	15.3	7.5	3.7	30.2	15.8
Vertisol	17.1	0.5	2.4	10.6	3.1	4.4	40.6	21.3

b)

Soil	I/S	P	I	K	Chl
Hamra	Major	-	Minor	Major	-
Loess	Major	Minor	Trace	Major	Trace
Vertisol	Dominant	Trace	-	Minor	Trace

Dominant: >60%, major: 20%-60%, minor: 5%-20%, trace: <5%

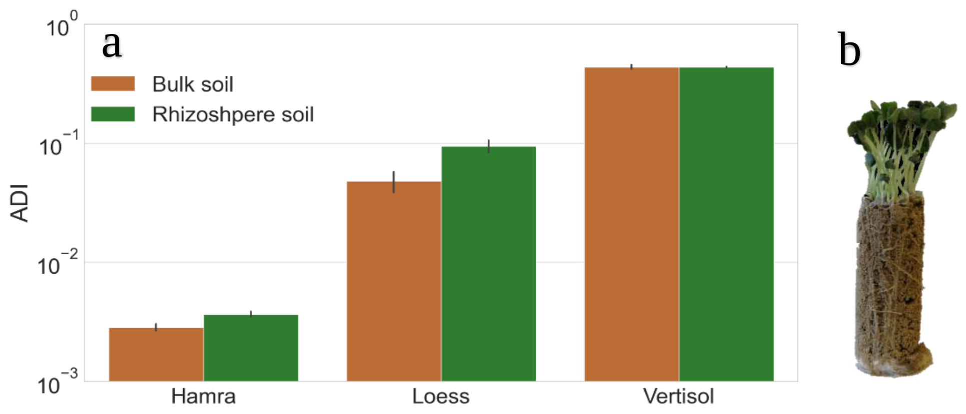

Figure 5: (a) ADI values for the soils before and after of *in-situ* Chia growth. (b) A side view of the Chia plant, soil and root system.

https://doi.org/10.5194/egusphere-2023-2501
Preprint. Discussion started: 10 November 2023

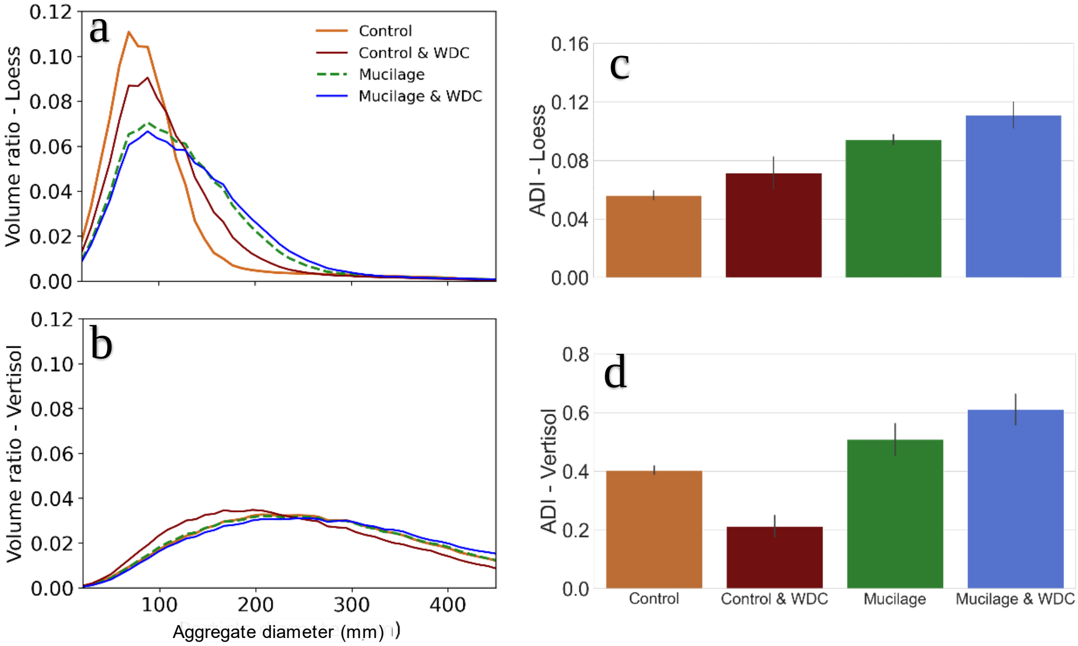

Figure 6: Aaggregate size distributions and ADI values of the (a,c) Loess and (b,d) Vertisol soils pre mucilage, pre mucilage with WDC, post mucilage and post mucilage with WDC.

580

https://doi.org/10.5194/egusphere-2023-2501
Preprint. Discussion started: 10 November 2023

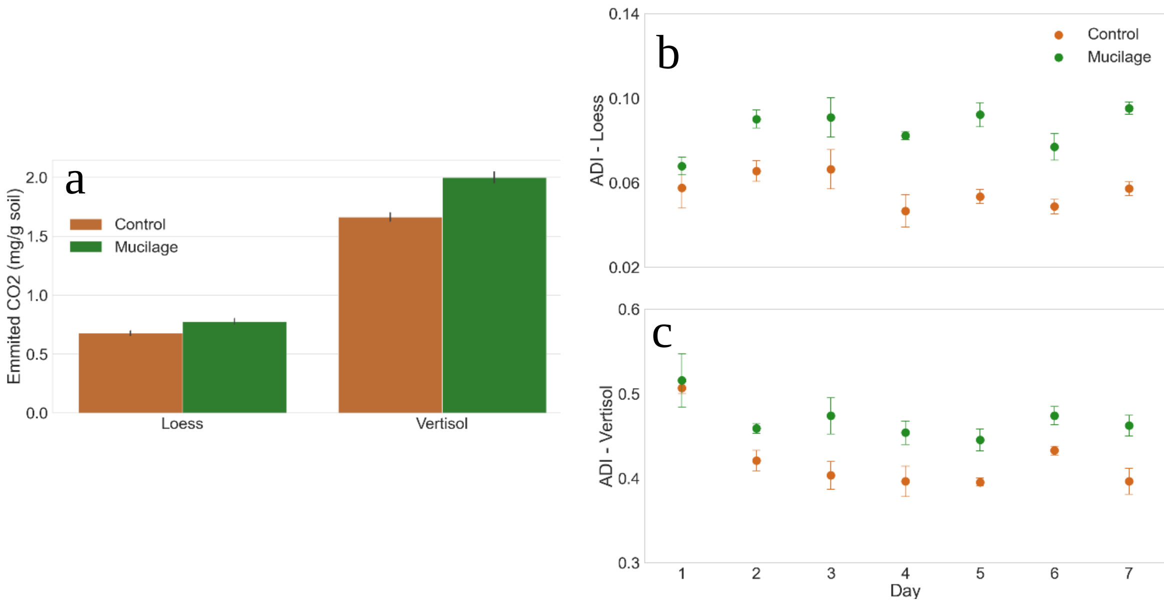

Figure 7: (a) Cumulative soil respiration values within 7 days and ADI values monitored for 7 days for (b) Loess and (c) Vertisol soils.